Bias Dependent TMR in Fe/MgO/Fe(100) Tunnel Junctions

Ivan Rungger[1], Alexandre Reily Rocha[1], Oleg Mryasov[2], Olle Heinonen[2], and Stefano Sanvito[1]
[1]School of Physics, Trinity College, Dublin, 2, Ireland
[2]Seagate Research, Pittsburgh, Pennsylvania, 15222

ABSTRACT

We calculate from first principles the *I-V* characteristics of Fe/MgO/Fe(100) tunnel junctions. In particular we compare the zero-bias transmission with self-consistent calculations at finite bias. In the case the magnetizations of the two Fe layers are parallel to each other, at small bias there is a significant contribution to the transmission coming from the minority spin channel. This is due to a sharp resonance in the transmission coefficient close to the Fermi level, originating from a surface state. As a bias exceeding 25 mV is applied, the surface states get out of resonance and the current through the minority spin channel saturates, so that the current flows mainly through the majority channel. The same effect is not present for the antiparallel alignment of the magnetization with the net result of large TMR at low bias, which then saturates for a bias larger than 25 mV.

INTRODUCTION

Fe/MgO/Fe(100) tunnel junctions have a large tunneling magnetoresistance (TMR) of up to 180% at room temperature [1,2]. Therefore these are promising candidates for device applications as magnetic read heads and MRAM. Theoretical spin-transport calculations in the linear response limit predict extremely large TMR values [3,4,5]. The calculations have shown that for thin junctions with only 4 MgO monolayers resonant surface states contribute significantly to the current at zero bias. Non-self-consistent calculations where the bias is introduced as a rigid shift of the density of states of the two magnetic electrodes predict a decrease of the TMR at very small bias [6]. This can be attributed to the surface states getting out of resonance. Here we investigate the current versus voltage behavior by calculating *self-consistently* the potential drop across the junction for an applied bias voltage. The dependence of the current through the surface states over the applied bias voltage is analyzed.

THEORY

The transport characteristics are studied with our newly developed code SMEAGOL [7]. SMEAGOL interfaces the non-equilibrium Green's functions (NEGF) method with density functional theory (DFT) using the numerical implementation contained in the SIESTA code [8]. The NEGF method splits up a two-terminal device into three regions, a semi-infinite left lead, a scattering region and a semi-infinite right lead. The key aspect is that it is possible to absorb the effects of the leads over the scattering region by means of the so-called self-energies Σ_L and Σ_R, respectively for the left and right lead. These are non-hermitian matrices. When added to the

Hamiltonian for the scattering region H_S, this describes the scattering region in the presence of the leads. The single particle Green's function for the scattering for one dimensional systems region is then

$$G(E,V) = [E\,S_S - H_S(V) - \Sigma_L(E,V) - \Sigma_R(E,V)]^{-1}, \tag{1}$$

where S_S is the overlap matrix of the scattering region, and the self-energies $\Sigma_{L/R}(E,V) = \Sigma_{L/R}(E \mp eV/2)$ are functions of the energy E and of the applied bias voltage V. A self-consistent procedure [7] can be designed to evaluate the actual form of the Hamiltonian H_S which in DFT depends on the non-equilibrium charge density and therefore on the voltage V. Once this is evaluated the transmission coefficient $T(E,V)$ for an applied voltage V is simply

$$T(E,V) = \mathrm{Tr}[\Gamma_L(E,V)\,G(E,V)^\dagger\,\Gamma_R(E,V)\,G(E,V)], \tag{2}$$

where

$$\begin{aligned}\Gamma(E,V)_L &= i\Big(\Sigma_L(E,V) - \Sigma_L(E,V)^\dagger\Big),\\ \Gamma(E,V)_R &= i\Big(\Sigma_R(E,V) - \Sigma_R(E,V)^\dagger\Big).\end{aligned} \tag{3}$$

The current $I(V)$ is then calculated as

$$I(V) = \frac{e}{h} \int_{-\infty}^{+\infty} dE\, T(E,V)\left(f\left(\frac{E - E_F - V/2}{k_B T}\right) - f\left(\frac{E - E_F + V/2}{k_B T}\right)\right), \tag{4}$$

where the function $f(x)$ is the Fermi-Dirac distribution function, k_B is the Boltzmann constant and T is the temperature.

If the system is periodic perpendicular to the transport direction (as is the case in the Fe/MgO/Fe(100) junction) then Bloch's theorem can be applied in the plane. All quantities given in equations (1)-(3) then depend on the wave vector $\mathbf{k} = (k_x, k_y)$ in the two-dimensional Brillouin zone (BZ) perpendicular to the transport direction. In particular the total transmission $T(E,V)$ is now obtained by integrating the k-point resolved transmission $T(E,V;k_x,k_y)$ over the BZ

$$T(E,V) = \frac{1}{\Omega_{BZ}} \int dk_x dk_y\, T(E,V;k_x,k_y), \tag{5}$$

where Ω_{BZ} is the area of the BZ.

We calculate the transmission properties for a Fe/MgO/Fe(100) junction where the MgO barrier is 4 monolayers thick. The coordinates used in our calculations are the same as in reference [3]. The SIESTA basis set for Fe is double zeta (DZ) for the s angular momentum (cutoff radius for the orbital $r_c = 7$ bohr), single zeta (SZ) for the p ($r_c = 7$ bohr), and DZ for the d ($r_c = 5.6$ bohr). For O and Mg the basis is DZP-s ($r_c = 6$ bohr), DZ-p ($r_c = 6$ bohr). The generalized gradient approximation (GGA) for the exchange correlation potential as parameterized in reference [9] has been used.

DISCUSSION

Zero bias voltage

In figure 1(a) the zero-bias transmission coefficient $T(E,V = 0)$ is shown for the parallel and antiparallel configuration of the Fe leads, and both the majority and minority spins (in the antiparallel case majority and minority refer to the magnetic orientation of the left lead). For the antiparallel configuration only the transmission for the majority is shown, since at 0 bias voltage majority and minority have the same transmission coefficient by symmetry. The transmission for the majority spin in the parallel case is approximately independent of the energy, whereas the minority has an enhanced transmission close to the Fermi energy. The peak in the transmission is due to a resonant surface state in the minority spin near the Fermi energy. Figure 1(b) shows the charge density for energies between −100 meV and +100 meV around the Fermi energy for majority and minority spins in the parallel configuration. The minority sub-band has an enhanced density located between the Fe and the first MgO layer, which corresponds to the surface state. Our results compare well with previous calculations [3,4]. We have however to consider that the actual position of the transmission peak is probably slightly different in all the three calculations. This may be due in part to the fact that in the present work the GGA is used for the exchange correlation potential, whereas in the previous works the local density approximation (LDA) was used. The two exchange and correlation functionals give a somewhat different band structure near the Fermi energy for Fe, and this probably results in a shift of the surface state with respect to E_F. In the antiparallel configuration the conductance is always lower than for the parallel configuration, but the signature of the surface state can again be found in a tiny enhancement of the transmission near the Fermi energy.
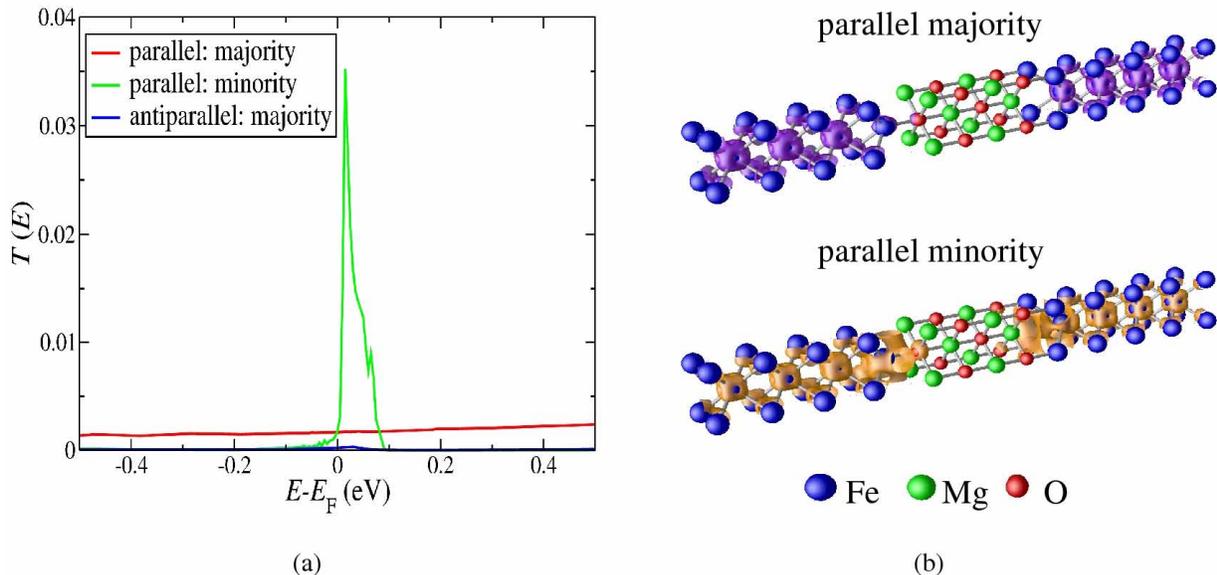

Figure 1. (a) Zero-bias transmission coefficient $T(E)$ as a function of energy E. (b) Charge density plot for states between −100 meV and +100 meV around the Fermi energy. Note the presence of a surface state for the minority spins.

In order to get a better understanding of the surface state, figure 2 shows the k-point resolved transmission coefficient $T(E, V = 0; k_x, k_y)$ as a function of k_x and k_y in the 2-dimensional Brillouin zone perpendicular to the transport direction for different energies. These range from -50 meV to -75 meV with respect to the Fermi energy. In the parallel configuration the majority spin (figure 2(a)) shows no dependence over the energy, whereas the minority (figure 2(b)) clearly shows the signature of the resonant surface state. In fact the figure demonstrates that the magnitude of the transmission depends strongly on the energy. Moreover it is also extremely sensitive to the actual k-point in the 2D Brillouin zone. The transmission coefficient for the antiparallel configuration (figure 2(c)) is essentially a convolution of that of the majority and that of the minority spin for the parallel alignment.
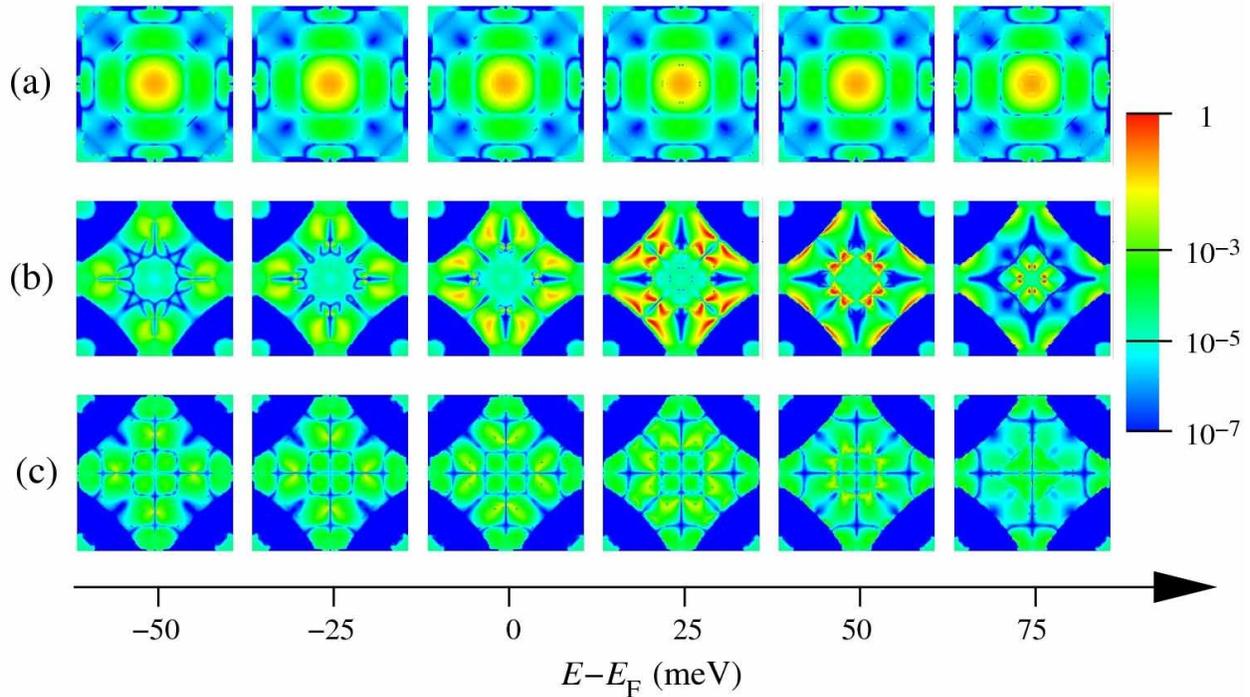

Figure 2. Transmission coefficient as a function of the k-vectors in the 2-dimensional Brillouin zone perpendicular to the transport direction. (a) parallel majority, (b) parallel minority, (c) antiparallel majority.

Finite bias voltage

Figure 3 shows the *I-V* curve for the parallel and antiparallel configurations of the leads, while in the inset we present the resulting TMR. For the majority spin in the parallel configuration there is an ohmic linear dependence of the current over the voltage. In contrast the minority spins give a large contribution to the current at bias voltages smaller than approximately 25 meV, and then the current saturates. This clearly shows that the large transmission in the minority spin channel is only found near zero-bias, when the surface states on both sides of the MgO spacer are in resonance. A small bias is sufficient to bring these states out of resonance.

In the antiparallel case the current rises up, although the slope decreases with bias. This indicates that the current mainly flows through the surface state. The saturation occurs when the

surface state is fully charged. The layer resistance at 100 mV is about 1 $\Omega\mu m^2$ for the parallel configuration, and 6 $\Omega\mu m^2$ for the antiparallel. To our knowledge there are no experimental values of the resistance for junctions thinner than about 6 MgO monolayers (ML) [1]. The value for 4 ML (the one calculated here) can be extrapolated from figure 2(b) of reference [1] to be about 6 $\Omega\mu m^2$ for both the parallel and for the antiparallel configurations. This value is of the same order of magnitude than that obtained in our calculations.

The inset of figure 3 shows the TMR as function of the applied bias. The TMR is defined as $TMR = (I_P - I_{AP})/I_{AP}$, where I_P is the current in the parallel configuration and I_{AP} is the current in the antiparallel configuration. For small biases the TMR is very large, exceeding 1500%, due to the contribution of the resonant transmission of the minority spin current in the parallel configuration. It then decreases and reaches a minimum value of just below 500% for a bias of about 60 mV. Finally the TMR rises again since the differential conductance is approximately constant for the parallel configuration, whereas it slowly decreases for the antiparallel. Experimentally the TMR for a 4 ML junction can be extrapolated from figure 2(c) of reference [1] to be of the order of 50%. This is smaller than our calculated value, that we have obtained assuming an ideal, perfectly epitaxial, junction. It is expected that in reality the presence of defects in the barrier and at the interface may decrease the device polarization and therefore the TMR. These effects are not included in our calculations.
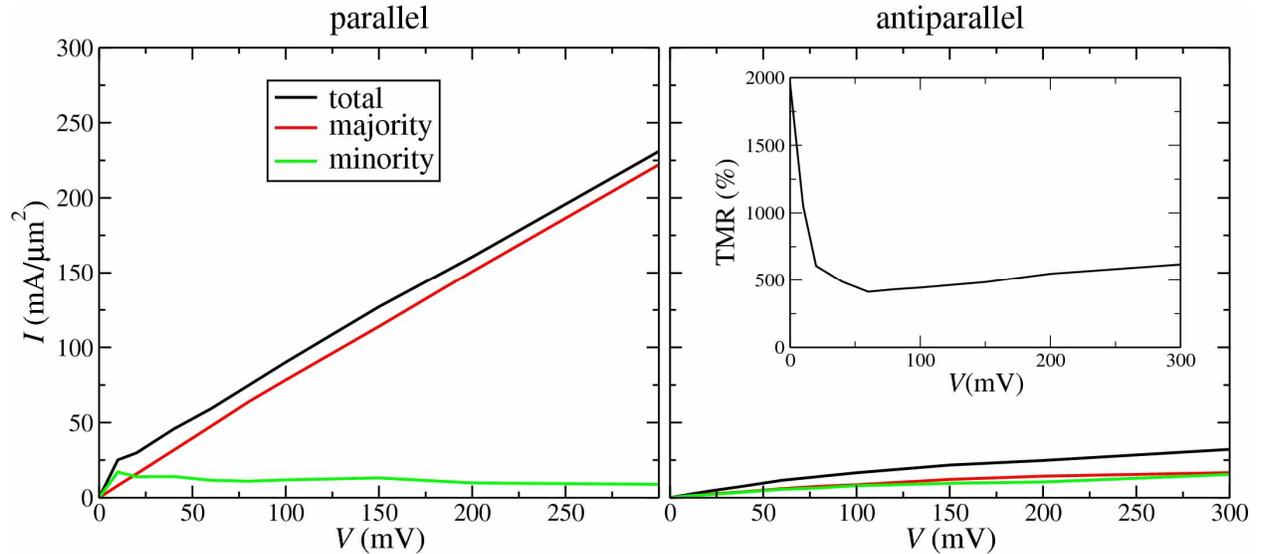

Figure 3. Current I versus voltage V for parallel and antiparallel configurations of the Fe leads. In the inset: TMR as function of voltage V.

CONCLUSIONS

We have calculated from first principles the *I-V* characteristics of an ideal Fe/MgO/Fe(100) tunneling junction. Our method allows us to evaluate self-consistently the potential drop across the junction, and therefore to follow the evolution of the surface states under bias. The calculated zero-bias transmission coefficient largely overestimates the contribution of the minority spins to the current in the parallel configuration. These contribute significantly to the current only up to bias voltages of about 25 mV, above which the surface states are out of resonance. This leads to an enhanced TMR at low bias voltages and to a saturation value of about 500% for *V* larger than 25 mV.

ACKNOWLEDGMENTS

REFERENCES

1. S. Yuasa, T. Nagahama, A. Fukushima, Y. Suzuki, and K. Ando, Nature Materials **3**, 868 (2004).
2. S. S. P. Parkin, C. Kaiser, A. Panchula, P. M. Rice, B. Hughes, M. Samant, and S.-H. Yang, Nature Materials **3**, 862 (2004).
3. W. H. Butler, X.-G. Zhang, T. C. Schulthess, and J. M. MacLaren, Phys. Rev. B 63, 054416 (2001).
4. K. D. Belashchenko, J. Velev, and E. Y. Tsymbal, Phys. Rev. B **72**, 140404(R) (2005).
5. D. Wortmann, G. Bihlmayer, and S. Blügel, J. Phys.: Condens. Matter **16**, S5819 (2004).
6. C. Heiliger, P. Zahn, B. Y. Yavorsky, and I. Mertig, Phys. Rev. B **72**, 180406(R) (2005).
7. A. R. Rocha, V. M. Garcia-Suarez, S. Bailey, C. Lambert, J. Ferrer, and S. Sanvito, Phys. Rev. B **73**, 085414 (2006); A. R. Rocha, V. M. Garcia-Suarez, S. Bailey, C. Lambert, J. Ferrer, and S. Sanvito, Nature Materials **4**, 335 (2005).
8. J. M. Soler, E. Artacho, J. D. Gale, A. Garcia, J. Junquera, P. Ordejon, and D. Sanchez-Portal, J. Phys.: Condens. Matter **14**, 2745 (2002).
9. J. P. Perdew, K. Burke, and M. Ernzerhof, Phys. Rev. Lett. **77**, 3865 (1996).